Angewandte Communications

Structured Peptides

DOI: 10.1002/anie.201((will be filled in by the editorial staff))

# Peptide ligands structured by small molecules**

*Shiyu Chen, Davide Bertoldo, Alessandro Angelini, Florence Pojer, and Christian Heinis**

***Abstract**: Bicyclic peptides evolved by phage display offer an attractive ligand format for the development of therapeutics. Being nearly 100-fold smaller than antibodies, they promise advantages such as access to chemical synthesis, efficient diffusion into tissues, and needle-free application. However, unlike antibodies, they do not have a folded structure in solution and thus bind less well. Herein, we developed bicyclic peptides with hydrophilic chemical structures at their center to promote non-covalent intra-molecular interactions, stabilizing the peptide conformation. The sequences of peptides isolated by phage display from large combinatorial libraries were strongly influenced by the type of small molecule used in the screen, suggesting that the peptides fold around the small molecules. X-ray structure analysis revealed that the small molecules indeed nucleated peptides by forming hydrogen bonds. The non-covalent interactions stabilize the peptide-protein complexes and contribute to the high binding affinity.*

Mimicking the binding site of antibodies by small synthetic molecules has been a longstanding challenge.[1] The binding contacts of antibodies are mediated by small regions at the tip of the Y-shaped structures, the so called complementarity determining regions (CDRs). In early attempts to generate synthetic antibody mimics, CDR-based peptide sequences were cyclized to stabilize the native conformation.[2] Later, multiple CDRs were anchored onto synthetic scaffolds.[1b,1c,3] The various constrained synthetic antibody mimics displayed improved binding affinities compared to individual linear CDR-based peptides. However, in all cases the affinities were significantly lower compared to those of the parental antibodies.

Good binders that structurally resemble rationally designed antibody mimics were obtained by screening billions of bicyclic peptides using phage display.[4] Bicyclic peptide libraries were generated by cyclizing cysteine-rich peptides displayed on phage with the thiol-reactive compound 1,3,5-tris(bromomethyl)benzene (TBMB).[4-5] Isolated bicyclic peptides bound with affinities in the nanomolar or even picomolar range and showed high target selectivity.[4, 6] A limitation of the bicyclic peptides is their rather flexible structure. 2D-NMR analysis of several phage-selected bicyclic peptides showed that they do not have a preferred three-dimensional folding in solution.[4,7] The high conformational flexibility prevents the development of binders to challenging targets such as peptides or small molecules, and it may limit the binding affinity of bicyclic peptides developed against tractable targets.

In this work, we raised the question if chemical linkers in bicyclic peptides could structure the peptide moiety by forming – in addition to the covalent bonds – non-covalent interactions with amino acids of the peptide (Figure 1a). More specifically, we wondered if the peptides anchored to small molecules and evolved in vitro for binding to protein targets would fold around the small molecules and deploy them as scaffolds. We chose to address this question by subjecting random peptides, covalently linked to various small molecules, to affinity selections against a protein target and analyzing the sequences and structures of isolated peptide ligands. We envisioned that non-covalent interactions could pre-organize the peptide loops to reduce the entropic penalty upon binding to the

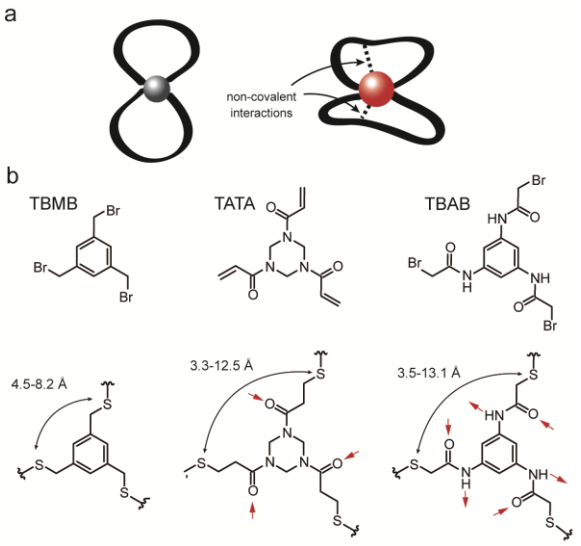


***Figure 1.*** Structurally diverse small molecules for phage selection of bicyclic peptides. a) Previously developed and structurally characterized bicyclic peptides were not structured by the central chemical linker illustrated by a grey ball (left). Small molecules with polar groups illustrated as red ball are envisioned to form H-bond interactions (black dashed lines) with the peptide loops and to serve as nucleating scaffolds (right). b) Structures of small molecules containing each three thiol-reactive groups before and after reaction. Potential H-bond donors and acceptors are indicated by red arrows. Computed distance ranges between the sulfur atoms of cyclized peptides are indicated.

[*] Dr. S. Chen, D. Bertoldo, Dr. A. Angelini, Prof. Dr. C. Heinis
Institute of Chemical Sciences and Engineering
Ecole Polytechnique Fédérale de Lausanne
CH-1015 Lausanne, Switzerland
E-mail: christian.heinis@epfl.ch
Dr. A. Angelini
David H. Koch Institute for Integrative Cancer Research
Massachusetts Institute of Technology (MIT)
Cambridge, MA 02139, USA
Dr. F. Pojer
Global Health Institute
Ecole Polytechnique Fédérale de Lausanne
CH-1015 Lausanne, Switzerland

[**] We thank Alice Tzeng for critical reading of this manuscript and the staff of beamlines PXIII and PXI of the SLS in Villigen, Switzerland, for their help. D. B, was kindly supported by the ITN Sphingonet. The financial contribution from the SNSF (Professorship PP00P3_123524/1 to C.H.) is gratefully acknowledged.

Supporting information for this article is available on the WWW under http://dx.doi.org/10.1002/anie.201xxxxxx.

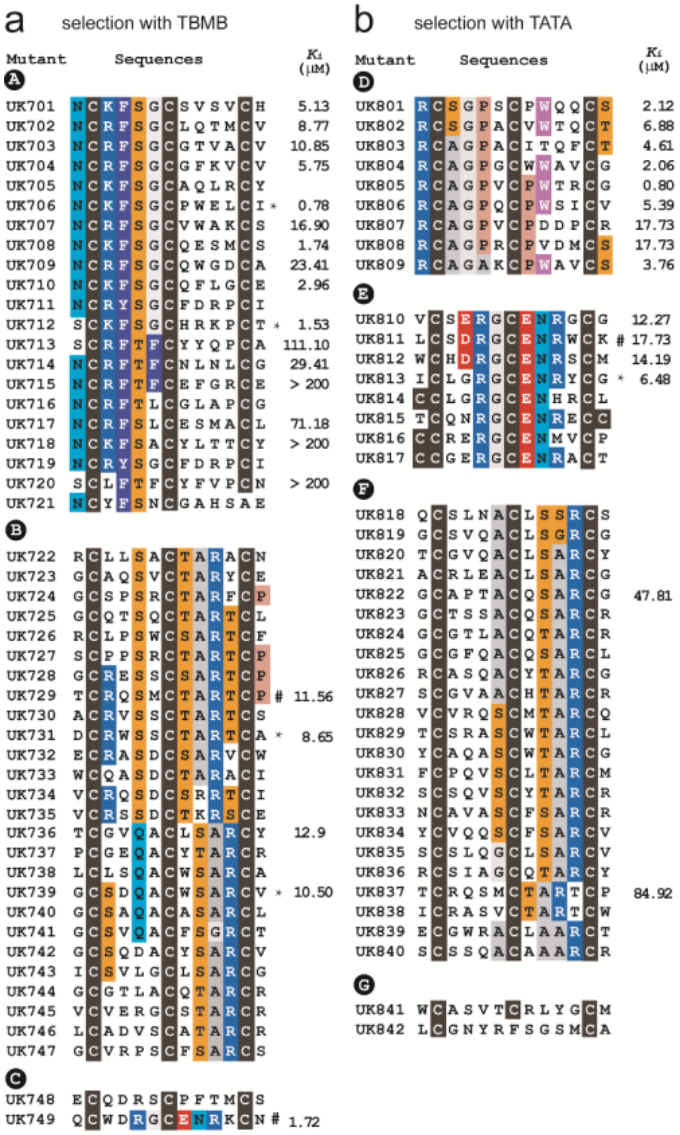


**Figure 2.** Peptides isolated in phage selections against uPA from the 4×4 library after cyclization with the chemical compounds TBMB (a), TATA (b) and TBAB (c). Peptides sharing similar sequences are arranged in groups and the similarities are highlighted in color. The indicated inhibition constants $K_i$ are averages of at least two measurements. Standard deviations were smaller than 20% in all cases and are not indicated. (*) Peptides were also cyclized with the other two chemical compounds (see Figure 3c). (#) Peptides were co-crystallized with uPA (see Figure 4).

target. Furthermore, we hoped that non-covalent interactions between peptide and a nucleating core could stabilize the peptide-target complex.

A recently solved first X-ray structure of a target-bound bicyclic peptide, UK18, inhibiting the serine protease urokinase-type plasminogen activator (uPA), showed that the central hydrophobic linker does not form non-covalent interactions with the peptide loops and thus does not serve as nucleating scaffold.[6a] To promote formation of hydrogen bonds between the small molecules and amino acids of the peptides, we applied in this work the hydrophilic small molecules 1,3,5-triacryloyl-1,3,5-triazinane (TATA) and *N*,*N*',*N*''-(benzene-1,3,5-triyl)-tris(2-bromoacetamide) (TBAB), each having multiple polar groups and three thiol-reactive groups (Figure 1b).[7] In parallel, we applied as a control also the small molecule TBMB,[4-5] the reagent that has a hydrophobic benzene ring at its center and previously proved not to serve as a nucleating scaffold in bicyclic peptides.[6a] The three small molecules have similar but different dimensions, holding the cysteines in cyclized peptides at different distances relative to each other (indicated in Figure 1b). The optimal concentration of small molecule reagent needed for the cyclization of peptides fused to the phage coat protein pIII were found to be 40 μM and 20 μM for TATA and TBAB, respectively (Figure S1a). Treatment of phage with the same or slightly higher concentrations of the compounds did not affect their infectivity (Figure S1b).

A peptide phage library of the format $XCX_4CX_4CX$-phage (4×4 library; X = any amino acid; library size $7.3\times10^8$) was reacted with the three thiol-reactive small molecules. The libraries were subjected to 2–3 iterative rounds of phage selection against human uPA, a protease involved in tumor growth and invasion.[8] The isolated peptides showed consensus sequences that were strongly biased by the small molecule structures linked to them (Figure 2). Most of the consensus sequences were found exclusively in selections with one of the three small molecules. Selections with TBMB yielded one unique consensus sequence (group A, Figure 2a), that with TATA two unique consensus sequences (group D and E, Figure 2b) and that with TBAB one unique consensus sequence (group H, Figure 2c). The consensus motifs 'TAR' and 'SAR' were found in selections with all three molecules (groups B, F and I in Figure 2). The same type of experiment was performed with a different peptide library of the format $XCX_3CX_3CX$-phage (3×3 library; library size $5.6\times10^8$). Also in this experiment, the consensus sequences of isolated peptides were strongly influenced by the small molecules used in the selections (Figure 3a), suggesting that the peptides fold closely around these structures or even form non-covalent interactions with them.

75 of the identified bicyclic peptides were synthesized and the inhibition of uPA measured (Figure 2a–c and 3a). Most inhibitors showed $K_i$s in the micromolar range and several in the high nanomolar range. In the selection with the 4×4 library, all three molecules yielded good binders ($K_i$s = 0.87–0.8 μM). In the selection with the 3×3 library, the by far best binders were isolated from pools of peptides cyclized with the new small molecule TBAB (best $K_i$ = 0.3 μM). Generation and testing of 20 mutants of one bicyclic peptide, UK805, yielded a 9-fold improved inhibitor (UK862; $K_i$ = 85 nM) (Figure 3b). This affinity is slightly weaker than that of the best bicyclic peptide inhibitor of uPA (UK202 containing the unnatural amino acid D-Ser; $K_i$ = 28 nM[9]) but it is

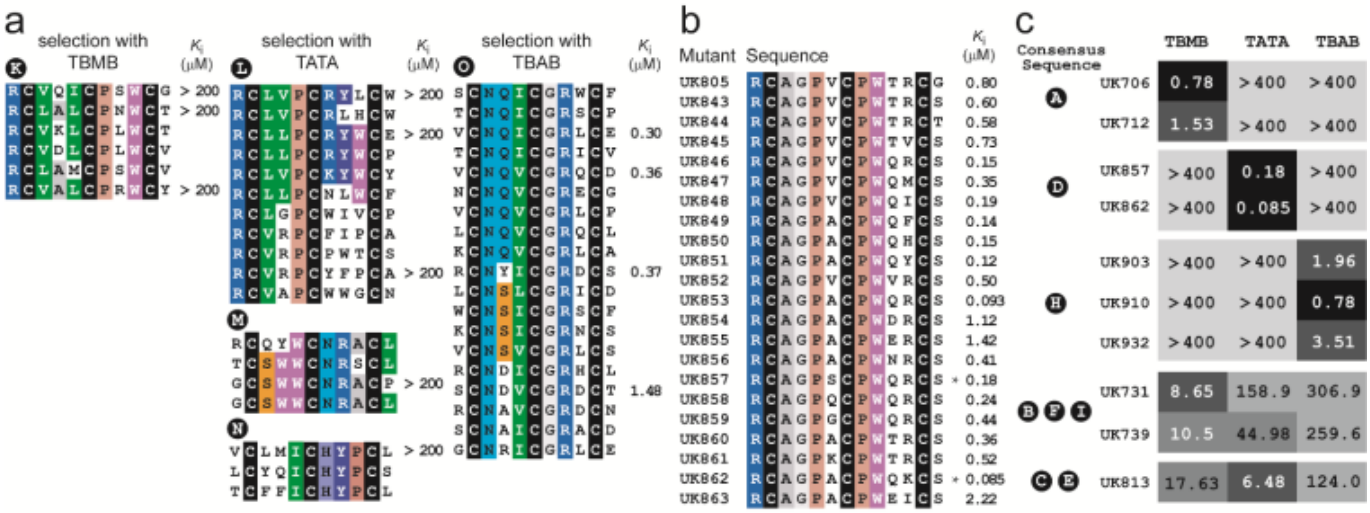


***Figure 3.*** Phage selected peptides and their activities. All indicated $K_i$s are averages of at least two measurements. Standard deviations were smaller than 20% in all cases and are not indicated. a) Peptides isolated in phage selections against uPA from the 3×3 library cyclized with the three chemical compounds. b) Affinity maturation of the peptide UK805 cyclized with TATA. c) Peptides tagged with an asterisk in Figure 2 and 3b were cyclized with all three small molecules and the $K_i$ for uPA measured.

remarkably good considering the short length of the peptide (13 amino acids vs. 17 amino acids in UK202).

To verify that the various consensus sequences indeed evolved due to the chemical and/or structural differences between the three small molecules, we swapped them in the best inhibitory peptides (Figure 3c; the peptides used are indicated with an asterisk in Figure 2a–c and 3b). Most peptides were found to be > 400-fold less active when cyclized with the two small molecules not used for phage selection. Peptides with the consensus motifs 'TAR' and 'SAR' found in selections with all three small molecules (for example UK731 and UK739; groups B, F and I), inhibited uPA when cyclized with any one of the three compounds. However, also for these peptides, the inhibitory activities were highest when the peptides were cyclized with the small molecule applied in the selection (Figure 3c). The swapping experiment proved that the peptides had adapted to the structural and chemical environment of the small molecules. Despite their comparable size, all three small molecules offer a different environment to the peptides.

Four out of around 50 tested bicyclic peptides co-crystallized with uPA and their structures could be determined at resolutions between 1.49 and 1.85 Å (Figure 4 and Figure S2; peptides indicated with hash symbols in Figure 2). Two of these peptides were cyclized by TBMB (UK729, PDB entry 4MNV; UK749, PDB entry 4MNW), one by TATA (UK811, PDB entry 4MNX) and one by TBAB (UK903, PDB entry 4MNY). As shown in Figure 4, the peptides bind in different orientations to the substrate-binding region of uPA.

In all the structures, the electron density of the small molecule was well resolved (Figure S2), allowing assignment of all atoms and identification of non-covalent interactions between small molecule and peptide (Figure S3–S5). In UK749, the mesitylene ring of TBMB does not form non-covalent interactions with amino acids of the peptide. In UK729, the mesitylene group of TBMB forms a hydrophobic contact with a small region of Gln4 but most of the mesitylene surface is entirely water-exposed. As found previously in the structure of the TBMB-cyclized bicyclic peptide UK18, the hydrophobic mesitylene core seems not to be an ideal scaffold to structure bicyclic peptides. In the bicyclic peptide UK811 cyclized with TATA, the triazinane structure did not form any non-covalent interactions with the peptide, despite its 3 potential H-bond donor groups. In contrast, in the bicyclic peptide UK903 cyclized with TBAB, having the largest number of polar groups, we found multiple non-covalent interactions between the small molecule and peptide. Specifically, the planar amide groups of TBAB form three H-bonds with amino acids of the peptide, namely with the side chain of Asn5 (H-bond distance: 3.08 Å), the carbonyl oxygen of Cys7 (H-bond distance: 2.93 Å) and the carbonyl oxygen of Val10 (H-bond distance: 3.12 Å) (Figure 5a-d). Peptide UK903 and TBAB form a dense structure with nearly no space in the interior that is accessible to water molecules (Figure 5e). The compactness and rigidity of the complex is underpinned by the exceptionally low B-factor values for the C-terminal 9 residues and benzenetriamide being in average 16.5 Å$^2$ compared to 19.6 Å$^2$ found for uPA in the co-crystal structure. The compact folding of UK903 resembles that of a protein.

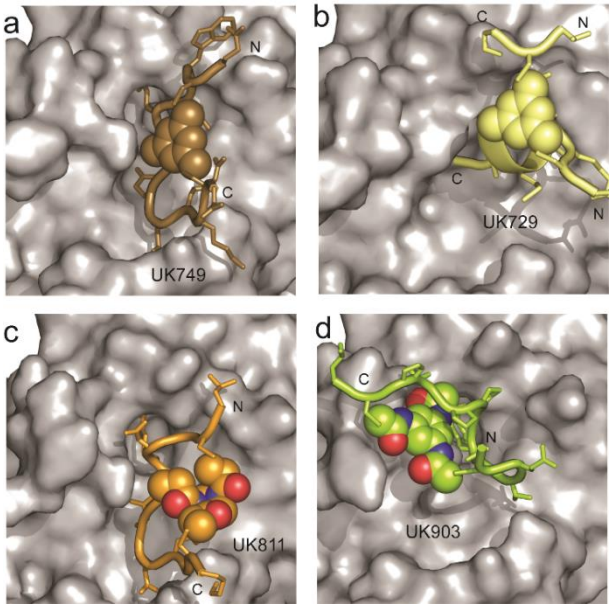


***Figure 4.*** Co-crystal structures of bicyclic peptides and uPA. The four peptides all bind to the active site of uPA (the same surface region of the protease is shown in all Figures). The chemical compound is shown as space fill model, the peptide backbone as tube and the side chains as sticks. Detailed structures are shown in Figure S2–S5. H-bond interactions are summarized in Tables S3–S10. a) UK749 cyclized with TBMB. b) UK729 cyclized with TBMB. The peptide is cleaved by uPA wherein the active site serine remains bound as acyl-enzyme intermediate to the C-terminus of the longer chain. c) UK811 cyclized with TATA. d) UK903 cyclized with TBAB.

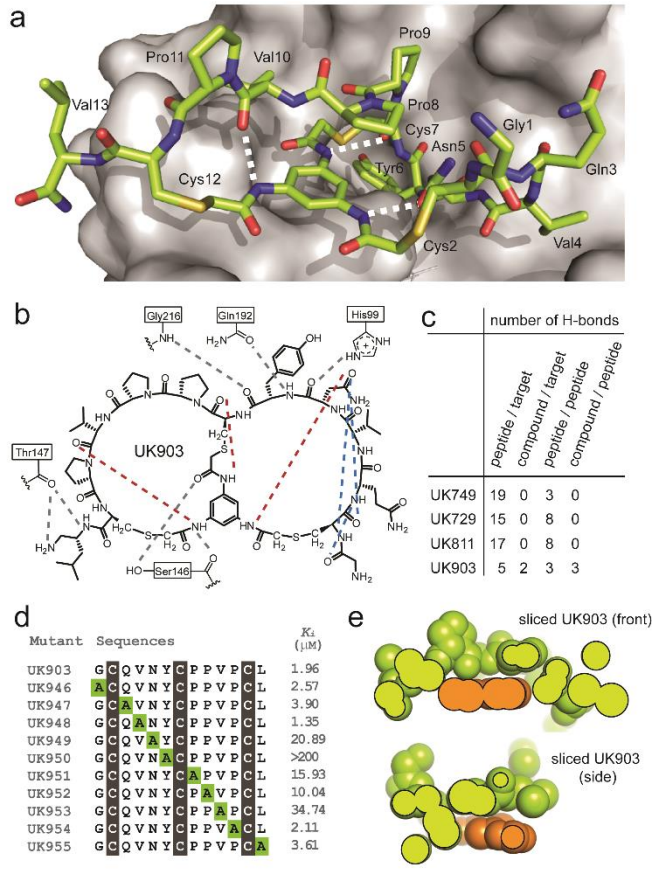


***Figure 5***. Structural properties of UK903. a) UK903 bound to uPA as a stick model. H-bonds between benzenetriamide core and peptide are shown as white dashed lines. b) Chemical structure of UK903 and H-bond interactions. c) Comparison of the number of H-bonds in the four bicyclic peptides co-crystallized with uPA. d) Alanine scan of UK903. e) UK903 represented as space fill model is sliced into two halves along perpendicular planes. The peptide is shown in green and the ring of TBAB in orange.

The finding that hydrophilic small molecules can form non-covalent interactions with peptides that are wrapped around them is of great interest as these contacts could potentially help stabilizing a three-dimensional structure in solution; this in turn could lower the entropic penalty upon binding to the target and result in higher binding affinities. We think that the observed 3 H-bonds between the peptide and the small molecule are likely not enough to stabilize the peptide into a defined structure in solution. However, the H-bonds might allow transient pre-organization of the peptide so that it resembles more its target-bound form and thus binds better than entirely flexible cyclic peptides. Undoubtedly, the H-bonds stabilize the complex between peptide and target protein as holds true for ligands with non-covalent intra-ligand interactions in general.

In summary, we demonstrate that it is possible to evolve peptides nucleated by small synthetic molecules and we show that polar molecules are most suited as cores and are superior to a hydrophobic structure previously used for the directed evolution of bicyclic peptides. The finding that small molecules can serve as structure-forming scaffolds paves the way for the generation of synthetic antibody-mimicking structures which has been a longstanding goal. The molecules combining a small size with excellent binding properties promise many advantages in clinical applications, including access to chemical synthesis, good tissue penetration and a range of administration options.

**Keywords:** antibody mimic • bicyclic peptide • macrocyclic ligands • peptides • phage display

[1] a) G. Vlatakis, L. I. Andersson, R. Muller, K. Mosbach, *Nature* **1993**, *361*, 645-647; b) M. Mutter, P. Dumy, P. Garrouste, C. Lehmann, M. Mathieu, C. Peggion, S. Peluso, A. Razzaname, G. Tuchscherer, *Angew. Chem., Int. Ed. Engl.* **1996**, *35*, 1482-1485; c) Y. Hamuro, M. C. Calama, H. S. Park, A. D. Hamilton, *Angew. Chem., Int. Ed. Engl.* **1997**, *36*, 2680-2683.

[2] a) H. U. Saragovi, D. Fitzpatrick, A. Raktabutr, H. Nakanishi, M. Kahn, M. I. Greene, *Science* **1991**, *253*, 792-795; b) M. Levi, M. Sallberg, U. Ruden, D. Herlyn, H. Maruyama, H. Wigzell, J. Marks, B. Wahren, *Proc. Natl. Acad. Sci. U. S. A.* **1993**, *90*, 4374-4378; c) M. Favre, K. Moehle, L. Y. Jiang, B. Pfeiffer, J. A. Robinson, *J. Am. Chem. Soc.* **1999**, *121*, 2679-2685; d) B. W. Park, H. T. Zhang, C. Wu, A. Berezov, X. Zhang, R. Dua, Q. Wang, G. Kao, D. M. O'Rourke, M. I. Greene, R. Murali, *Nat. Biotechnol.* **2000**, *18*, 194-198.

[3] P. Timmerman, R. Barderas, J. Desmet, D. Altschuh, S. Shochat, M. J. Hollestelle, J. W. Hoppener, A. Monasterio, J. I. Casal, R. H. Meloen, *J. Biol. Chem.* **2009**, *284*, 34126-34134.

[4] C. Heinis, T. Rutherford, S. Freund, G. Winter, *Nat. Chem. Biol.* **2009**, *5*, 502-507.

[5] P. Timmerman, J. Beld, W. C. Puijk, R. H. Meloen, *Chembiochem* **2005**, *6*, 821-824.

[6] a) A. Angelini, L. Cendron, S. Chen, J. Touati, G. Winter, G. Zanotti, C. Heinis, *ACS Chem. Biol.* **2012**, *7*, 817-821; b) V. Baeriswyl, S. Calzavarini, C. Gerschheimer, P. Diderich, A. Angelillo-Scherrer, C. Heinis, *J. Med. Chem.* **2013**, *56*, 3742-3746; c) I. R. Rebollo, A. Angelini, C. Heinis, *Medchemcomm* **2013**, *4*, 145-150.

[7] S. Chen, J. Morales-Sanfrutos, A. Angelini, B. Cutting, C. Heinis, *Chembiochem* **2012**, *13*, 1032-1038.

[8] P. A. Andreasen, R. Egelund, H. H. Petersen, *Cell. Mol. Life Sci.* **2000**, *57*, 25-40.

[9] S. Chen, D. Gfeller, S. A. Buth, O. Michielin, P. G. Leiman, C. Heinis, *Chembiochem* **2013**, *14*, 1316-1322.

Angewandte Communications

**Entry for the Table of Contents**

## *Structured Peptides*

Shiyu Chen, Davide Bertoldo, Alessandro Angelini, Florence Pojer, and Christian Heinis*

_____ **Page – Page**

Peptide ligands structured by small molecules

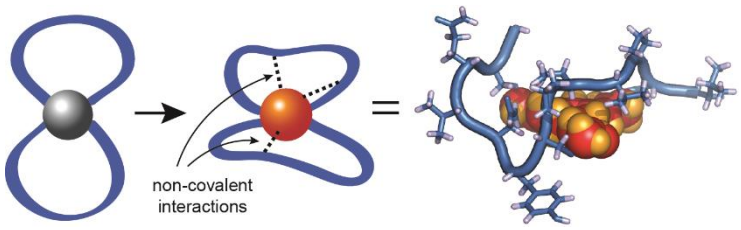


Bicyclic peptide ligands evolved by phage display provide an attractive format for the development of therapeutics but their flexible conformation limits the binding affinity. We found that small hydrophilic molecules at the center of bicyclic peptides can form non-covalent interactions with amino acids of the peptides and thus stabilize their conformation and strengthen the binding interaction. Our results recommend polar compounds as ideal molecular scaffolds for the development of synthetic antibody-mimicking structures.

## Supplementary Information

# Mimicking antibodies by peptides that fold around small molecules

Shiyu Chen[1], Davide Bertoldo[1], Alessandro Angelini[1†], Florence Pojer[2], and Christian Heinis[1]*

[1] Institute of Chemical Sciences and Engineering, [2] Global Health Institute, Ecole Polytechnique Fédérale de Lausanne, CH-1015 Lausanne, Switzerland

[†] Present address: David H. Koch Institute for Integrative Cancer Research, Massachusetts Institute of Technology (MIT), Cambridge, MA 02139, USA

* Corresponding author

E-mail address: christian.heinis@epfl.ch

**Supplementary Materials and Methods**

*Calculation of small molecule dimensions*

The structures of all three small molecules reacted with methanethiol were constructed and the geometries optimized with Gaussian09 using the Hartree-Fock method and the 6-31g(d) basis set with a water solvent reaction field. The minimized structures were parameterized with a general AMBER force field (GAFF) before subjection to a dynamic run in Amber11 with GPU accelerated PMEMD. The distances between the sulfurs were calculated from a simulation of at least 20 ns. All the calculation was performed in the ELECTRA cluster provided by EPFL.

*Expression and purification of peptide-pIII(1-217) fusion protein*

The fusion protein comprising the N-terminal peptide $^{N}$AACSYSEGWCKEYLELCG$^{C}$, the linker GSG, the disulfide-free domains D1 and D2 of the M13 phage gene 3 protein[1] (amino acids 1 to 217), the linker KLAAALE and a hexa-histidine tag was expressed in *E. coli* (strain BL21 (DE3) Codon Plus) using the cytoplasmic expression vector pET-28b(+) (Merck Novagen, Nottingham, UK). Bacteria growing in 500 ml 2YT media in a shaking flask were induced with 0.5 mM IPTG at $OD_{600}$ = 0.6 and incubated overnight at 25 °C. Cells were pelleted by centrifugation (8000 rpm, 20 min, 4 °C) and resuspended in buffer containing lysozyme (30 mM sodium phosphate, pH 7.4, 300 mM NaCl, 10 mM imidazole, 1 mM TCEP with 0.1% v/v Triton X-100, 50 μg/mL DNase and 100 μg/mL lysozyme). The cells were additionally sonicated and the protein was purified stepwise by Ni-affinity chromatography and gel filtration. In the Ni-affinity chromatography, the column (HiTrap™ FF 1 ml column, GE Healthcare, Uppsala, Sweden) was washed with buffer containing 30 mM sodium phosphate, pH 7.4, 300 mM NaCl, 10 mM imidazole and 1 mM TCEP, and eluted with buffer containing 30 mM sodium phosphate, pH 7.4, 300 mM NaCl, 500 mM imidazole and 1 mM TCEP. In the gel filtration (HiPrep™ 16/60 Sephacryl™ S-100 column, GE Healthcare, Uppsala, Sweden), a buffer containing 20 mM $NH_4HCO_3$, pH 8.0, 5 mM EDTA and 10 μM TCEP buffer was used. The purification process was performed on an ÄKTAxpress system (GE Healthcare, Glattbrugg, Switzerland). A 0.5 litre culture yielded 23 mg of purified fusion protein with a mass of 27636 Da being 17 Da larger than its expected mass (27619.05 Da).

*Cyclization of peptide fused to phage pIII*

Peptide $^{N}$AACSYSEGWCKEYLELCG$^{C}$ fused to pIII(1-217) (20 μM) was reduced in degassed reaction buffer (20 mM $NH_4HCO_3$, 5 mM EDTA, pH 8.0) by addition of TCEP (1 mM) and incubation at 42 °C for 1 hr. The concentration of TCEP was reduced by size exclusion chromatography using a PD-10 desalting column and degassed reaction buffer (20 mM $NH_4HCO_3$, 5 mM EDTA, pH 8.0). The protein (2 μM) was incubated with 0, 10, 20, 40 or 80 μM TBMB, TATA or TBAB in 20% v/v acetonitrile and 80% v/v degassed reaction buffer at 30 °C for 1 hr and quenched with 300 μM free cysteine. Modified protein was concentrated to 5-20 μM by filtration (Microcon® Ultracel YM-3, regenerated cellulose 3000 MWCO; Millipore, Carrigtwohill, Co. Cork, Ireland). The molecular mass of the peptide-pIII(1-217) fusion protein before and after reaction was measured by electrospray ionisation mass spectrometry (ESI-MS) on a quadrupole time-of-flight mass spectrometer (Q-TOF).

*Phage infectivity measurement*

The number of infective phage was determined as follows: 12 serial dilutions (10-fold) of the reactions were prepared using 2YT medium. 20 μl of each dilution was added to 180 μl exponentially growing TG1 cells ($OD_{600}$ = 0.4) and incubated for 90 minutes at 37 °C. 20 μl of the infected TG1 cells were spot onto 2YT agar plates containing 30 μg/ml chloramphenicol. The number of colonies was counted the next day and the number of infective phage was calculated.

*Protease inhibition assay*

The inhibition constants $K_i$s were determined by incubating different concentrations of bicyclic peptide with fixed concentration of human uPA (1.5 nM; activated catalytic domain; expressed in mammalian cells as described before[2]). The enzymatic assays were performed at 25 °C using the fluorogenic substrate Z-Gly-Gly-Arg-AMC (50 μM; Bachem, Bubendorf, Switzerland) in 10 mM Tris-Cl, pH 7.4, 150 mM NaCl, 10 mM $MgCl_2$, 1 mM $CaCl_2$, 0.1% w/v BSA, 0.01% v/v Triton-X100 buffer. The uPA activity was measured by monitoring the change in fluorescence intensity (excitation at 368 nm, emission recorded at 467 nm) during 30 minutes with 1 min interval using a fluorescence plate reader (Tecan Infinite M200 Pro, Switzerland). $K_i$s were determined by correcting for the competitive effect of the substrate

$[S]_0$ using the equation $K_i = IC_{50}/(1+[S]/K_m)$. The $K_m$ for the hydrolysis of Z-Gly-Gly-Arg-AMC by human uPA was 122 μM.

*Expression and purification of the catalytic domain of human uPA*

The mutated catalytic domain of human uPA being deficient of an unpaired cysteine and an asparagine glycosylation site (uPA-C122A/N145Q) was expressed in mammalian cells as follows. The suspension-adapted HEK-293 cells were grown in serum-free ExCell 293 medium (100 mL; SAFC Biosciences, St. Louis, MO) in the presence of 4 mM glutamine and the histone deacetylase inhibitor valproic acid (3.75 mM; 2-propylypentanoic acid, sodium salt or VPA) in an orbitally shaken bottle at 180 rpm in an ISF-4-W incubator (Kühner AG, Birsfelden, Switzerland) at 37° C in the presence of 5% $CO_2$. The pSecTagA-LMWuPA-C122A/N145Q plasmid was transfected into embryonic kidney cells (HEK-293) at high cell density ($20 \times 10^6$ cells/mL) using linear polyethylenimine (PEI, Polysciences, Eppenheim, Germany). At the end of the 7-day production phase, cells were harvested by centrifugation at 2500 rpm for 15 min at 4 °C. Any additional cell debris was removed from the medium by filtration through 0.45 μm PES membranes (Filter-top 250 mL low protein binding TPP). Medium containing the recombinant human uPA was adjusted to pH 6.5 with diluted HCl and concentrated in a 10,000 MWCO Vivaspin-20 ultrafiltration unit (Sartorius-Stedim Biotech GmbH). The filtration unit was spun at 4000 rpm on a Heraeus Multifuge 3L-R centrifuge (Thermo Scientific, Germany) at 4 °C until one fourth of starting volume was reached. The concentrate was diluted with cooled water to two times of the starting supernatant volume and the pH was adjusted to 6.5 with diluted HCl. The recombinant human uPA was captured on 2 mL strong cation exchange SP sepharose fast flow resin (GE Healthcare). The diluted medium was passed through the pre-equilibrated resin at a flow rate of 1 mL/min at 4 °C using a peristaltic pump. The column was connected to an AKTApurifier system (GE Healthcare). After extensive washing with buffer B (25 mM sodium phosphate pH 6.4), recombinant human uPA was eluted with buffer C (25 mM sodium phosphate, 500 mM NaCl, pH 6.4) by applying a linear gradient of 0 to 100% over 30 minutes. Fractions containing human uPA were pooled, concentrated in a 10,000 MWCO Vivaspin-20 ultrafiltration unit as before. The concentrated protein was subjected to gel filtration on a Superdex 75 10/300 GL column (GE Healthcare) equilibrated with buffer D (50 mM HEPES, 150 mM NaCl, pH 8.0) connected to an AKTApurifier system. The protein was eluted as a monomer giving a single band in SDS-PAGE, with an apparent molecular mass of about 32 kDa. Human uPA was

converted into its active two-chain form by plasmin cleavage. The protease removed the N-terminal sixteen amino acid residues of the A-chain (K136-K158 in the HMW human uPA numbering). To a solution of 45 μM LMW human uPA-C122A/N145Q in buffer D, 90 nM plasmin (HPLM, from human plasma, 85 kDa, Molecular Innovations) was added (molar ratio 500:1). After incubation for 4 hours at 25 °C, the activated protein was purified by size exclusion chromatography using a Superdex 75 10/300 GL column and buffer E (50 mM HEPES, 100 m NaCl, pH 7.0, degassed) on an AKTApurifier system. The protein was eluted as a monomer. SDS-PAGE under reducing conditions showed a single band with a molecular mass of about 28 kDa, confirming quantitative activation of uPA. The pure and activated LMW uPA-C122A/N145Q in buffer E was concentrated to 20 mg/mL for crystallization by using a 10,000 MWCO Vivaspin-20 ultrafiltration tube as described above. The protein was frozen and stored at -80 °C.

## Supplementary Tables

| | Phage selection (small molecule/target) | | | |
|---|---|---|---|---|
| **Selection round** | **TBMB/uPA** | **TBMB/no target** | **TATA/uPA** | **TBAB/uPA** |
| 1 | $5.60 \times 10^5$ | $1.75 \times 10^4$ | $9.80 \times 10^5$ | $1.29 \times 10^6$ |
| 2 | $1.32 \times 10^8$ | $1.05 \times 10^5$ | $5.95 \times 10^8$ | $2.83 \times 10^8$ |
| 3 | $1.40 \times 10^9$ | $7.00 \times 10^4$ | $1.68 \times 10^9$ | $1.92 \times 10^9$ |

**Supplementary Table S1.** Titers of phage isolated in the three rounds of panning with the 4×4 library against uPA. The peptide library was cyclized with the three indicated small molecules. For the library cyclized with TBMB, a selection omitting the target protein was performed as negative control. The number of phage isolated against uPA increased in the 2$^{nd}$ and 3$^{rd}$ round compared to the negative control, indicating that uPa-specific peptides were enriched.

| **Data collection *** | **UK749/uPA** | **UK729/uPA** | **UK811/uPA** | **UK903/uPA** |
|---|---|---|---|---|
| Number of images | 600 | 600 | 600 | 900 |
| Oscillation degree | 0.2º | 0.2º | 0.2º | 0.2º |
| Wavelength | 1 Å | 1 Å | 1 Å | 1 Å |
| Space group | $P2_12_12_1$, # 19 | $P2_12_12_1$, # 19 | $P2_12_12_1$, # 19 | P 1 $2_1$ 1, # 4 |
| Cell dimensions | | | | |
| a, b, c (Å), | 52.57, 53.96, 80.17 | 52.31, 54.06, 79.67 | 52.45, 53.50, 79.58 | 67.96, 54.46, 71.68 |
| Asymmetric unit content | 1 | 1 | 1 | 2 |
| Resolution (Å) | 44.76 – 1.49 | 44.73 – 1.80 | 44.40 – 1.85 | 45.68 – 1.70 |
| $R_{merge}$ | 0.132 (0.183) | 0.187 (0.592) | 0.124 (0.621) | 0.065 (0.386) |
| $\langle I / \sigma I \rangle$ | 8.1 (5.7) | 5.2 (2.9) | 6.3 (2.0) | 10.5 (2.5) |
| Completeness (%) | 96.2 (98.4) | 95.2 (95.6) | 98.1 (97.7) | 98.6 (92.5) |
| Redundancy | 3.8 (3.8) | 4.0 (3.9) | 3.9 (3.8) | 3.3 (2.8) |
| **Refinement** | | | | |
| No. reflections | | | | |
| Working | 34787 | 19293 | 18289 | 53950 |
| Test | 1811 | 1029 | 990 | 2847 |
| $R_{work}$ / $R_{free}$ | 0.1515/0.1630 | 0.1889/0.2052 | 0.1892/0.2164 | 0.1572/0.1916 |
| B factor ($Å^2$) | 19.77 | 27.95 | 26.82 | 20.48 |
| R.m.s. deviations | | | | |
| Bond lengths (Å) | 0.005 | 0.007 | 0.008 | 0.007 |
| Bond angles (°) | 1.120 | 1.279 | 1.359 | 1.376 |
| No. atoms | | | | |
| Protein | 1939 | 1934 | 1934 | 3876 |
| Peptide inhibitor | 119 | 106 | 125 | 226 |
| Solvent | 170 | 113 | 125 | 434 |
| Ramachandran plot (%) | | | | |
| Most favoured + additionally allowed | 100 | 99.5 | 99.5 | 99.5 |
| Outliers | 0 | 0.5 | 0.5 | 0.5 |

**Supplementary Table S2.** Data collection and refinement statistics. Rotations of 0.2° were performed. (*) 1 crystal was used to collect all diffraction data. Highest-resolution shell is shown in parentheses.

| Residue/atoms 1 | Residue/atoms 2 | Distance (Å) |
|---|---|---|
| Asp4 OD1 | Gly6 N | 3.00 |
| Arg5 O | Cys7 N | 3.00 |
| Glu8 O | Arg10 N | 3.30 |

**Supplementary Table S3.** Intra-molecular hydrogen bonds in UK749.

| UK749 residue/atoms | Human uPA residue/atoms | Distance (Å) |
|---|---|---|
| Trp3 O | Gly218 N | 2.85 |
| Asp4 OD2 | His99 NE2 | 3.14 |
| Arg5 N | Gly216 O | 3.00 |
| Arg5 NE | Gly218 O | 2.81 |
| Arg5 NH2 | Gly218 O | 3.06 |
| Arg5 NH2 | Asp189 OD2 | 2.85 |
| Arg5 NH1 | Asp189 OD2 | 3.27 |
| Arg5 NH1 | Asp189 OD1 | 2.89 |
| Arg5 NH1 | Ser190OG | 2.83 |
| Gly6 O | His99 NE2 | 3.12 |
| Glu8 OE1 | His57 NE2 | 2.71 |
| Glu8 OE1 | Ser195 OG | 2.99 |
| Glu8 OE2 | Ser195 OG | 2.72 |
| Glu8 OE2 | Gly193 N | 2.70 |
| Asn9 OD1 | Arg35 NE | 2.81 |
| Asn9 OD1 | Arg35 NH2 | 3.06 |
| Asn9 ND2 | Cys58 O | 2.81 |
| Asn9 ND2 | Tyr64 OH | 3.06 |
| Lys11 N | Asp60A OD2 | 2.90 |

**Supplementary Table S4.** Hydrogen bonds between UK749 and uPA.

| Residue/atoms 1 | Residue/atoms 2 | Distance (Å) |
|---|---|---|
| Arg3 O | Met6 N | 3.03 |
| Gln4 O | Cys7 N | 2.75 |
| Gln4 O | Thr8 N | 3.04 |
| Gln4 NE2 | Thr11 O | 2.96 |
| Ser5 O | Thr8 OG1 | 3.14 |
| Ser5 O | Ala9 N | 3.16 |
| Ser5 O | His99 NE2 | 2.78 |
| Thr8 O | Arg10 N | 3.25 |

**Supplementary Table S5.** Intra-molecular hydrogen bonds in UK729.

| UK729 residue/atoms | Human uPA residue/atoms | Distance (Å) |
|---|---|---|
| Ser5 N | Thr97A O | 2.87 |
| Ser5 OG | Asp97 O | 2.71 |
| Cys7 O | Gln192 NE2 | 3.09 |
| Thr8 O | Gly216 N | 3.00 |
| Thr8 OG1 | Leu97B O | 2.69 |
| Thr8 OG1 | His99 NE2 | 3.28 |
| Ala9 O | Gln192 NE2 | 2.86 |
| Arg10 O | Gly193 N | 2.86 |
| Arg10 O | Ser195 N | 2.88 |
| Arg10 N | Ser214 O | 2.96 |
| Arg10 NH2 | Gly218 O | 2.81 |
| Arg10 NH2 | Asp189 OD2 | 2.8 |
| Arg10 NH1 | Asp189 OD1 | 2.92 |
| Arg10 NH1 | Ser190 O | 3.13 |
| Arg10 NH1 | Ser190 OG | 2.73 |

**Supplementary Table S6.** Hydrogen bonds between UK729 and uPA.

| Residue/Atoms 1 | Residue/Atoms 2 | Distance (Å) |
|---|---|---|
| Ser3 OG | Arg5 O | 2.45 |
| Asp4 O | Gly6 N | 3.15 |
| Asp4 O | Cys7 N | 2.96 |
| Gly6 N | Glu8 OE2 | 2.97 |
| Gly6 O | Arg10 NH1 | 2.86 |
| Cys7 N | Asp4 O | 2.96 |
| Glu8 O | Arg10 N | 3.26 |
| Glu8 OE2 | Ser195 OG | 3.09 |

**Supplementary Table S7.** Intra-molecular hydrogen bonds in UK811.

| UK811 residue/atoms | Human uPA residue/atoms | Distance (Å) |
|---|---|---|
| Ser3 OG | Gly216 O | 2.73 |
| Ser3 OG | Gly216 N | 2.96 |
| Arg5 NH2 | Gly218 O | 2.87 |
| Arg5 NH2 | Asp189 OD2 | 2.92 |
| Arg5 NH1 | Asp189 OD1 | 2.97 |
| Arg5 NH1 | Asp189 OD2 | 3.28 |
| Arg5 NH1 | Ser190 O | 3.11 |
| Arg5 NH1 | Ser190 OG | 2.75 |
| Glu8 OE1 | Gly193 N | 2.75 |
| Glu8 OE1 | Ser195 OG | 2.58 |
| Glu8 OE2 | His57 NE2 | 2.76 |
| Asn9 OD1 | Arg35 NH2 | 2.83 |
| Asn9 ND2 | Tyr64 OH | 3.12 |
| Asn9 ND2 | Cys58 O | 2.75 |
| Arg10 NE | Asp60A OD2 | 2.93 |
| Arg10 NH1 | Gly6 O | 2.86 |
| Trp11 N | Asp60A OD2 | 2.79 |

**Supplementary Table S8.** Hydrogen bonds between UK811 and uPA.

| Residue/Atoms 1 | Residue/Atoms 2 | Distance (Å) |
|---|---|---|
| Gly1 O | Gln3 N | 3.01 |
| Cys2 O | Asn5 ND2 | 2.76 |
| Cys2 N | Asn5 OD1 | 3.13 |
| Asn5 OD1 | TBA15 N1 | 3.08 |
| Cys7 O | TBA15 N2 | 2.93 |
| Val10 O | TBA15 N3 | 3.12 |

**Supplementary Table S9.** Intra-molecular hydrogen bonds in UK903.

| UK903 residue/atoms | Human uPA residue/atoms | Distance (Å) |
|---|---|---|
| Asn5 O | His99 NE2 | 2.85 |
| Tyr6 N | Gln192 OE1 | 2.83 |
| Tyr6 O | Gly216 N | 3.05 |
| Leu13 N | Thr147 O | 2.86 |
| Amide N | Thr147 O | 3.16 |
| TBA15 O2 | Ser146 OG | 2.84 |
| TBA15 N3 | Ser146 O | 2.82 |

**Supplementary Table S10.** Hydrogen bonds between UK903 and uPA.

| Peptide/compound | Sequence | Calculated mass | Measured mass |
|---|---|---|---|
| UK701/TBMB | NCKFSGCSVSVCH | 1483.63 | 1484.3 |
| UK702/TBMB | NCRFSGCLQTMCV | 1574.67 | 1575.6 |
| UK703/TBMB | NCRFSGCGTVACV | 1429.62 | 1429.6 |
| UK704/TBMB | NCRFSGCGFKVCV | 1532.70 | 1532.5 |
| UK706/TBMB | NCKFSGCPWELCI | 1612.71 | 1613.9 |
| UK706/TATA | NCKFSGCPWELCI | 1747.78 | 1747.3 |
| UK706/TBAB | NCKFSGCPWELCI | 1741.73 | 1741.5 |
| UK707/TBMB | NCRFSGCVWAKCS | 1573.69 | 1573.6 |
| UK708/TBMB | NCKFSGCQESMCS | 1536.57 | 1537.2 |
| UK709/TBMB | NCRFSGCQWGDCA | 1559.60 | 1559.5 |
| UK710/TBMB | NCKFSGCQFLGCE | 1548.64 | 1548.3 |
| UK712/TBMB | SCKFSGCHRKPCT | 1566.71 | 1566.5 |
| UK712/TATA | SCKFSGCHRKPCT | 1695.73 | 1695.1 |
| UK712/TBAB | SCKFSGCHRKPCT | 1701.78 | 1701.1 |
| UK713/TBMB | SCRFTFCYYQPCA | 1701.70 | 1701.4 |
| UK714/TBMB | NCRFTFCNLNLCG | 1617.71 | 1617.8 |
| UK715/TBMB | NCRFTFCEFGRCE | 1724.71 | 1724.4 |
| UK717/TBMB | NCRFSLCESMACL | 1589.67 | 1589.7 |
| UK718/TBMB | NCKFSACYLTTCY | 1629.69 | 1629.4 |
| UK720/TBMB | SCLFTFCYFVPCN | 1656.70 | 1656.7 |
| UK729/TBMB | TCRQSMCTARTCP | 1570.67 | 1570.8 |
| UK731/TBMB | DCRWSSCTARTCA | 1572.65 | 1572.8 |
| UK731/TATA | DCRWSSCTARTCA | 1707.71 | 1707.8 |
| UK731/TBAB | DCRWSSCTARTCA | 1701.67 | 1701.7 |
| UK736/TBMB | TCGVQACLSARCY | 1487.66 | 1487.9 |
| UK739/TBMB | GCSDQACWSARCV | 1498.60 | 1498.0 |
| UK739/TATA | GCSDQACWSARCV | 1633.67 | 1633.6 |
| UK739/TBAB | GCSDQACWSARCV | 1627.62 | 1627.5 |
| UK749/TBMB | QCWDRGCENRKCN | 1724.72 | 1725.0 |
| UK801/TATA | RCSGPSCPWQQCS | 1686.70 | 1686.9 |
| UK802/TATA | RCSGPACVWTQCT | 1659.72 | 1659.9 |
| UK803/TATA | RCAGPACITQFCT | 1618.73 | 1619.5 |
| UK804/TATA | RCAGPGCWWAVCG | 1613.69 | 1614.7 |
| UK805/TATA | RCAGPVCPWTRCG | 1653.76 | 1653.2 |
| UK806/TATA | RCAGPQCPWSICV | 1667.76 | 1669.0 |

| | | | |
|---|---|---|---|
| UK807/TATA | RCAGPVCPDDPCR | 1636.71 | 1636.3 |
| UK808/TATA | RCAGPRCPVDMCS | 1642.71 | 1642.8 |
| UK809/TATA | RCAGAKCPWAVCS | 1599.73 | 1600.4 |
| Uk810/TATA | VCSERGCENRGCG | 1617.67 | 1618.2 |
| Uk811/TATA | LCSDRGCENRWCK | 1817.80 | 1819.0 |
| Uk812/TATA | WCHDRGCENRSCM | 1844.72 | 1845.3 |
| Uk813/TATA | ICLGRGCENRYCG | 1691.76 | 1692.6 |
| Uk813/TBMB | ICLGRGCENRYCG | 1556.69 | 1556.5 |
| Uk813/TBAB | ICLGRGCENRYCG | 1685.71 | 1685.4 |
| UK822/TATA | GCAPTACQSARCG | 1472.62 | 1472.8 |
| UK837/TATA | TCRQSMCTARTCP | 1705.74 | 1705.7 |
| UK901/TBAB | GCVPQYCPPPLCG | 1575.65 | 1575.3 |
| UK902/TBAB | KCQGSYCPPVACL | 1610.69 | 1610.7 |
| UK903/TBAB | GCQVNYCPPVPCL | 1634.69 | 1634.4 |
| UK903/TBMB | GCQVNYCPPVPCL | 1505.67 | 1505.1 |
| UK903/TATA | GCQVNYCPPVPCL | 1640.74 | 1640.1 |
| UK904/TBAB | QCQVSYCPPVRCD | 1739.71 | 1740.2 |
| UK905/TBAB | GCAVSYCPPQFCN | 1630.62 | 1630.2 |
| UK906/TBAB | MCHVSYCPWQGCT | 1756.65 | 1756.4 |
| UK907/TBAB | RCMVSYCPEIGCT | 1703.68 | 1703.3 |
| UK908/TBAB | QCSVSYCPQVPCQ | 1683.67 | 1683.4 |
| UK910/TBAB | GCFPSYCPQVACQ | 1644.64 | 1644.7 |
| UK910/TBMB | GCFPSYCPQVACQ | 1515.62 | 1515.2 |
| UK910/TATA | GCFPSYCPQVACQ | 1650.69 | 1650.1 |
| UK911/TBAB | GCGPSYCPQVACQ | 1554.59 | 1554.6 |
| UK913/TBAB | RCGPSYCPDDFCF | 1751.64 | 1751.5 |
| UK914/TBAB | FCGPSYCPYTGCA | 1610.59 | 1610.5 |
| UK915/TBAB | GCGPSYCSYVPCG | 1534.55 | 1534.4 |
| UK916/TBAB | VCQTSYCPYVPCL | 1717.72 | 1717.5 |
| UK917/TBAB | YCQASYCPGVPCR | 1688.68 | 1688.6 |
| UK919/TBAB | DCA-SYCPFVECV | 1577.59 | 1577.1 |
| UK922/TBAB | WCQAEYCAFVPCI | 1774.72 | 1774.4 |
| UK923/TBAB | QCQAEYCPRVRCT | 1798.76 | 1798.5 |
| UK924/TBAB | RCQGEYCPPVRCL | 1765.77 | 1765.3 |
| UK925/TBAB | SCQGEYCPFVVCE | 1705.64 | 1705.4 |
| UK926/TBAB | WCQPEYCPQSGCD | 1757.61 | 1757.4 |
| UK927/TBAB | GCQVEYCPPVPCL | 1649.69 | 1649.4 |

| | | | |
|---|---|---|---|
| UK928/TBAB | SCQAQYCPEVQCR | 1756.70 | 1756.9 |
| UK929/TBAB | NCQPQYCPRVTCI | 1766.76 | 1766.7 |
| UK930/TBAB | ECQPQYCPSVGCK | 1683.67 | 1683.7 |
| UK931/TBAB | VCQGQYCPPVECS | 1654.64 | 1654.5 |
| UK932/TBAB | GCQVQYCPPVPCL | 1648.71 | 1648.5 |
| UK932/TBMB | GCQVQYCPPVPCL | 1519.69 | 1519.3 |
| UK932/TATA | GCQVQYCPPVPCL | 1654.75 | 1654.2 |
| UK933/TBAB | GCFPQYCPMMPCV | 1717.65 | 1717.7 |
| UK843/TATA | RCAGPVCPWTRCS | 1683.77 | 1684.2 |
| UK844/TATA | RCAGPVCPWTRCT | 1697.78 | 1698.2 |
| UK845/TATA | RCAGPVCPWTVCS | 1626.73 | 1627.0 |
| UK846/TATA | RCAGPVCPWQRCS | 1710.78 | 1710.9 |
| UK847/TATA | RCAGPVCPWQMCS | 1685.72 | 1686.3 |
| UK848/TATA | RCAGPVCPWQICS | 1667.76 | 1668.5 |
| UK849/TATA | RCAGPACPWQFCS | 1673.71 | 1674.4 |
| UK850/TATA | RCAGPACPWQHCS | 1663.70 | 1664.3 |
| UK851/TATA | RCAGPACPWQYCS | 1689.71 | 1690.6 |
| UK852/TATA | RCAGPVCPWVRCS | 1681.79 | 1682.1 |
| UK853/TATA | RCAGPACPWQRCS | 1682.75 | 1683.5 |
| UK854/TATA | RCAGPACPWDRCS | 1669.71 | 1670.1 |
| UK855/TATA | RCAGPACPWERCS | 1683.73 | 1684.1 |
| UK856/TATA | RCAGPACPWNRCS | 1668.73 | 1669.6 |
| UK857/TATA | RCAGPSCPWQRCS | 1698.74 | 1699.3 |
| UK858/TATA | RCAGPQCPWQRCS | 1739.77 | 1740.3 |
| UK859/TATA | RCAGPGCPWQRCS | 1668.73 | 1669.3 |
| UK860/TATA | RCAGPACPWTRCS | 1655.74 | 1656.1 |
| UK861/TATA | RCAGPKCPWTRCS | 1712.79 | 1713.1 |
| UK862/TATA | RCAGPACPWQKCS | 1654.74 | 1655.3 |
| UK863/TATA | RCAGPACPWEICS | 1640.71 | 1641.6 |
| UK946/TBAB | ACQVNYCPPVPCL | 1648.71 | 1648.4 |
| UK947/TBAB | GCAVNYCPPVPCL | 1577.67 | 1577.3 |
| UK948/TBAB | GCQANYCPPVPCL | 1606.66 | 1606.3 |
| UK949/TBAB | GCQVAYCPPVPCL | 1591.69 | 1591.2 |
| UK950/TBAB | GCQVNACPPVPCL | 1542.67 | 1542.2 |
| UK951/TBAB | GCQVNYCAPVPCL | 1608.68 | 1608.3 |
| UK952/TBAB | GCQVNYCPAVPCL | 1608.68 | 1608.2 |
| UK953/TBAB | GCQVNYCPPAPCL | 1606.66 | 1606.2 |

| | | | |
|---|---|---|---|
| UK954/TBAB | GCQVNYCPPVACL | 1608.68 | 1608.3 |
| UK955/TBAB | GCQVNYCPPVPCA | 1592.64 | 1592.3 |

**Supplementary Table S11.** Masses of synthesized peptides. All peptides were synthesized on solid phase with rink amide MBHA resin and have an amidated C-terminus. The correct mass of each peptide was verified by MALDI-TOF without calibration for each individual peptide. The calculated and experimental masses are indicated.

**Supplementary Figures**

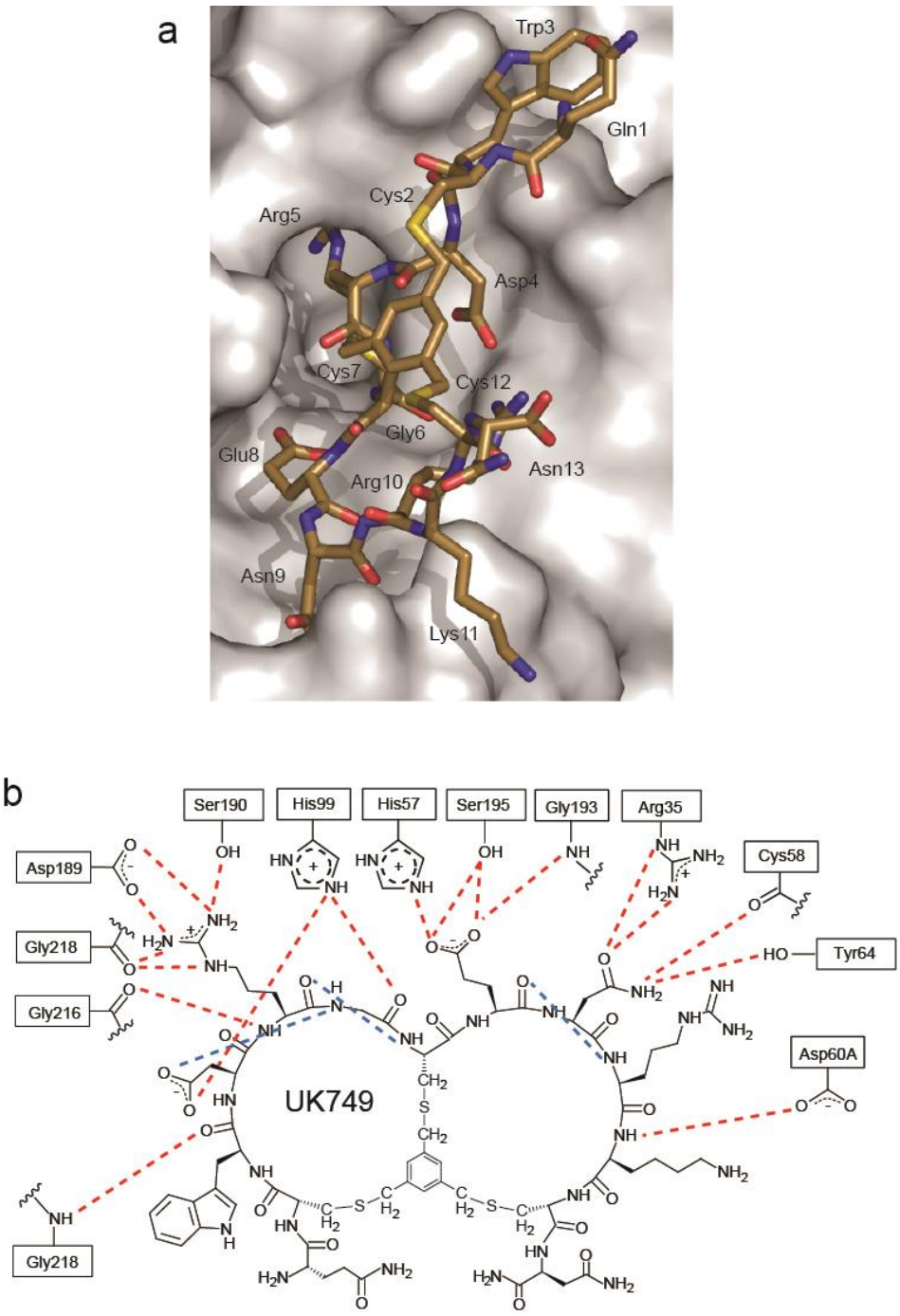


**Supplementary Figure S1.** Structure of UK749 bound to uPA (PDB entry 4MNW). (a) X-ray structure with UK749 shown as stick model. (b) Chemical structure of UK749. H-bond interactions (dashed lines) between the bicyclic peptide and uPA (red), and in between amino acids of the peptide (blue) are indicated.

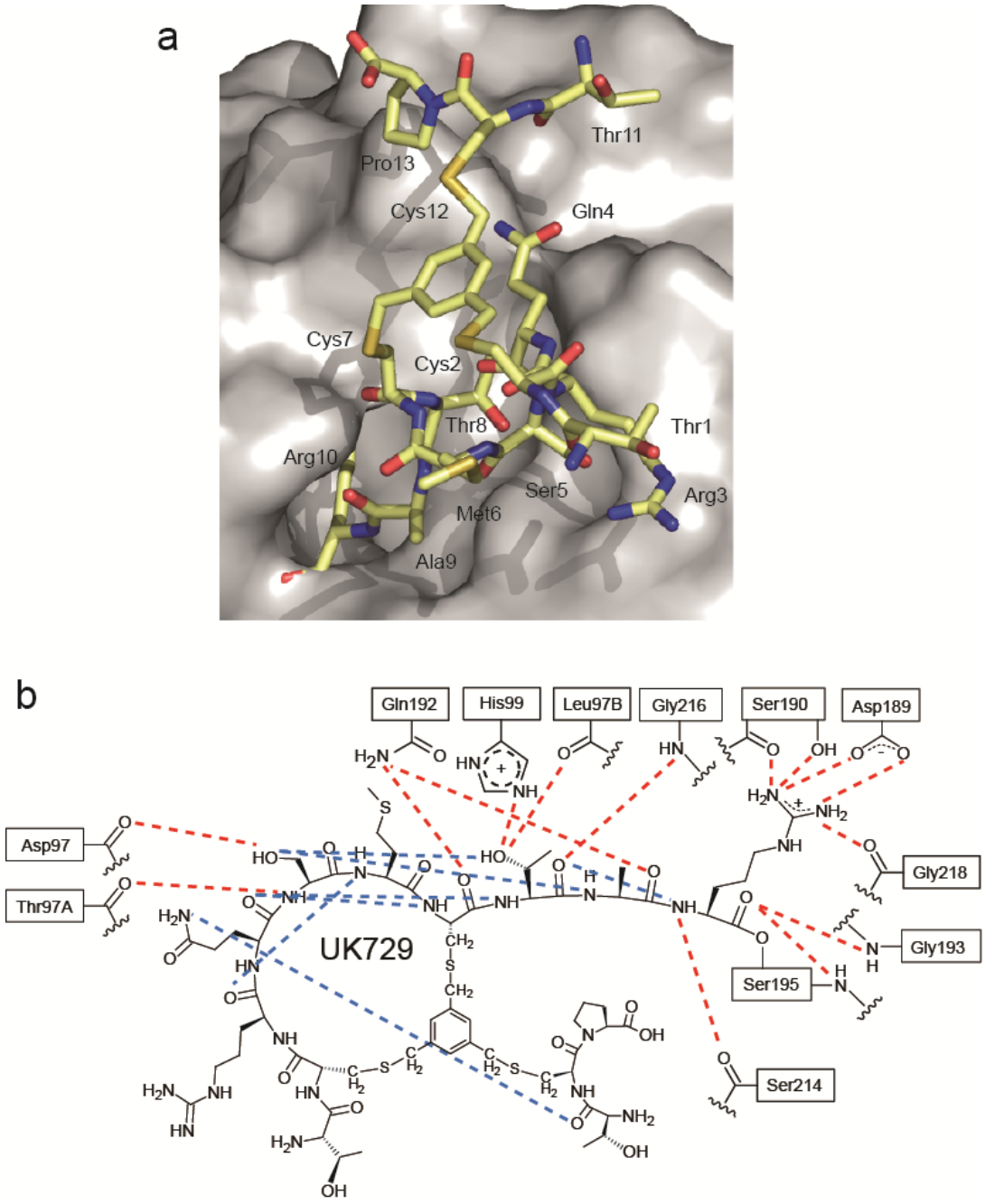


**Supplementary Figure S2.** Structure of UK729 bound to uPA (PDB entry 4MNV). (a) X-ray structure with UK729 shown as stick model. (b) Chemical structure of UK729. H-bond interactions (dashed lines) between the bicyclic peptide and uPA (red), and in between amino acids of the peptide (blue) are indicated.

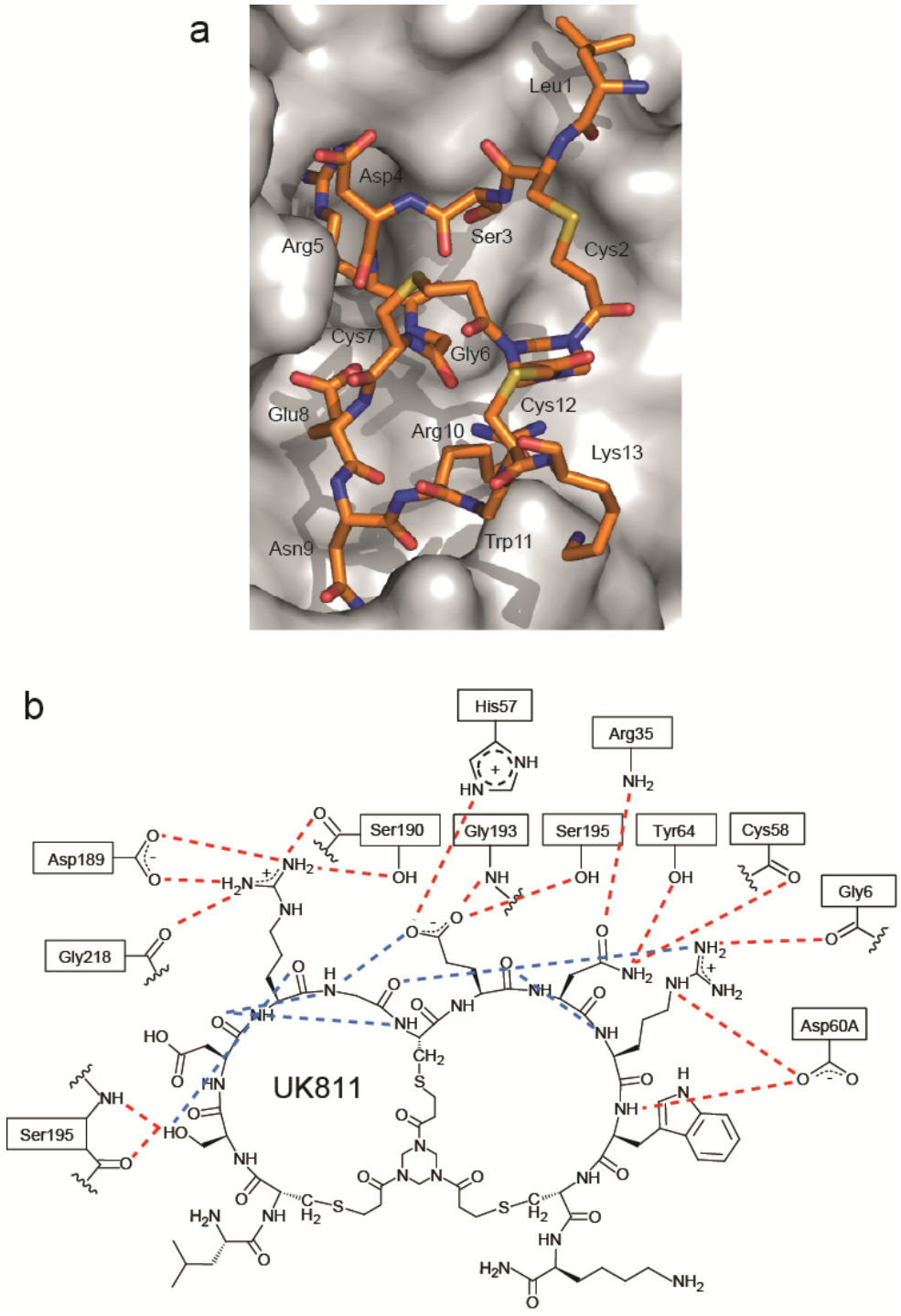


**Supplementary Figure S3.** Structure of UK811 bound to uPA (PDB entry 4MNX). (a) X-ray structure with UK811 shown as stick model. (b) Chemical structure of UK811. H-bond interactions (dashed lines) between the bicyclic peptide and uPA (red), and in between amino acids of the peptide (blue) are indicated.

## References


1. Kather I, Bippes CA, Schmid FX. A stable disulfide-free gene-3-protein of phage fd generated by in vitro evolution. *J Mol Biol* 2005, **354**(3)**:** 666-678.

2. Angelini A, Cendron L, Chen S, Touati J, Winter G, Zanotti G, *et al.* Bicyclic Peptide Inhibitor Reveals Large Contact Interface with a Protease Target. *ACS Chemical Biology* 2012, **7**(5)**:** 817-821.